Title: Metabolomics study of *Populus* type propolis

Author: Boban Anđelković Ljubodrag Vujisić Ivan Vučković Vele Tešević Vlatka Vajs Dejan Gođevac

PII: S0731-7085(16)30493-9
DOI: http://dx.doi.org/doi:10.1016/j.jpba.2016.12.003
Reference: PBA 10968

To appear in: *Journal of Pharmaceutical and Biomedical Analysis*

Received date: 1-9-2016
Revised date: 1-12-2016
Accepted date: 3-12-2016

Please cite this article as: Boban Anđelković, Ljubodrag Vujisić, Ivan Vučković, Vele Tešević, Vlatka Vajs, Dejan Gođevac, Metabolomics study of Populus type propolis, Journal of Pharmaceutical and Biomedical Analysis http://dx.doi.org/10.1016/j.jpba.2016.12.003

Metabolomics study of *Populus* type propolis

Boban Anđelković[a], Ljubodrag Vujisić[a], Ivan Vučković[a], Vele Tešević[a], Vlatka Vajs[b], Dejan Gođevac*[b]

Affiliation:

[a]Faculty of Chemistry, University of Belgrade, Studentski trg 12-16, 11000 Belgrade, Serbia

[b]Institute of Chemistry, Technology and Metallurgy, University of Belgrade, Studentski trg 12-16, 11000 Belgrade, Serbia

*Corresponding author

Dejan Gođevac

Institute of Chemistry, Technology and Metallurgy, University of Belgrade, 11000 Belgrade, Serbia

E-mail: dgodjev@chem.bg.ac.rs Phone: + 381 11 2630474 Fax: + 381 112636061

Graphical abstract

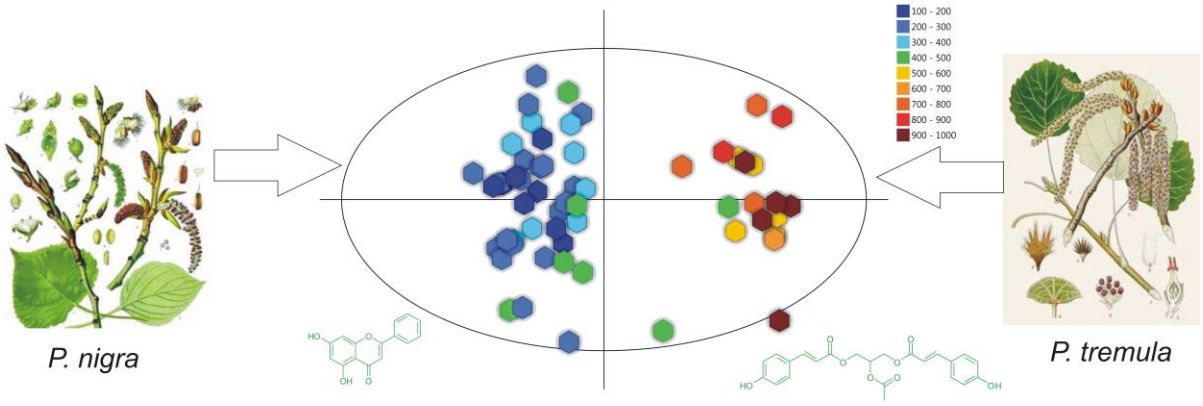

Highlights

- Altitude variability in *Populus* type propolis composition is investigated.
- NMR, IR, and UV spectroscopy methods in combination with OPLS are applied.
- Botanical origin of propolis is determined.
- An O2PLS method is used to integrate spectral data of propolis and *Populus* buds.

Abstract

Herein, we propose rapid and simple spectroscopic methods to determine the chemical composition of propolis derived from various *Populus* species using a metabolomics approach. In order to correlate variability in *Populus* type propolis composition with the altitude of its collection, NMR, IR, and UV spectroscopy followed by OPLS was conducted. The botanical origin of propolis was established by comparing propolis spectral data to those of buds of various *Populus* species. An O2PLS method was utilized to integrate two blocks of data. According to OPLS and O2PLS, the major compounds in propolis samples, collected from temperate continental climate above 500 m, were phenolic glycerides originating from *P. tremula* buds. Flavonoids were predominant in propolis samples collected below 400 m, originating from *P. nigra* and *P. x euramericana* buds. Samples collected at 400-500 m were of mixed origin, with variable amounts of all detected metabolites.

Keywords propolis; NMR; IR; UV; OPLS; O2PLS

1. Introduction

Propolis is produced by honey bees as a result of mixing wax and botanical material, such as buds, saps, and plant resins. For bees, propolis has a protective role: it seals small holes and cracks in the hive, which helps with defense against microorganisms, insects, and adverse weather conditions. It has been used in traditional medicine since ancient times. Its antimicrobial, antiviral, antioxidant, anti-inflammatory, anti-ulcer, immunostimulating, and antitumor properties are well-documented [1]. Nowadays, propolis is still in use in folk medicine, as it was the case in the last centuries. Moreover, it is now used as a natural food additive, as a functional foods ingredient, and as a constituent of natural cosmetics [2,3].

As the botanical sources of propolis collection strongly depend on specific geographical location and climate, there is great variation in its chemical composition [4]. Buds of *Populus* species are the main source of propolis in temperate climates, including in Europe, North America, Asia, South America, and New Zealand [2,5]. There are two main types of propolis from *Populus* species, varying considerably in chemical composition. The most widespread and the most studied is the one originating from buds of black poplar (*P. nigra* L., from section *Aigeiros*), which contains characteristic flavonoids, such as chrysin, galangin, pinocembrin, pinobanksin, pinobanksin-3-O-acetate, and pinocembrin chalcone [2,6]. Another type of propolis was found to contain phenolic

glycerides, characteristic of aspen buds (*P. tremula* L., from section *Leuce*) in Europe, or American aspen (*P. tremuloides* Michx., from section *Leuce*) in North America [6]. The composition of propolis is of great importance for quality control in companies that produce propolis-based preparations, because corresponding biological effects are strongly dependent on the type of compounds present. Since propolis has highly complex chemical composition, with more than 300 compounds detected, comprehensive qualitative and quantitative determination of all compounds is impractical [4,7]. There are numerous reports on chromatography-based techniques for propolis component profiling, such as LC-MS [8-16] or GC-MS methods [17-26], which are not cost-effective and time-consuming [27]. On the other hand, spectroscopic methods, without prior chromatographic separation of the components, are underappreciated as a tool for propolis classification. Thus, Watson et al. applied ^{1}H NMR spectroscopy, in combination with principal components analysis, to differentiate between propolis originating from Europe, Africa, Asia, Solomon Islands, and Brazil. It should be noted from their results that propolis from various parts of the world could have considerable differences in chemical composition [28]. In other studies, the authors used ^{1}H NMR [27] and UV-Vis spectroscopy [29] for propolis classification associated with seasonal variations and different regions of Brazil. NIR spectroscopy has been applied for geographical origin discrimination and flavonoid content determination of propolis from different regions of China [30]. Simultaneous recognition of flavonoids and free phenolic acids, characteristic for the black poplar type of propolis, has been accomplished by ^{1}H NMR [31,32]. HPLC-PDA, HPLC-MS, and ^{1}H NMR have been used to distinguish between the brown, red, and yellow Cuban varieties of propolis [33]. According to the HPTLC fingerprint technique, authors recently detected the presence of two main types of poplar propolis, called “orange” and “blue” [34-39]. By TLC-MS analysis, “orange” type propolis appeared to be similar to those of black poplar, while the “blue” type showed a similar profile to aspen [4].

Herein, we propose rapid and simple methods for the determination of propolis chemical composition derived from various *Populus* species using a metabolomics approach. For this purpose, NMR, IR, and UV spectroscopic methods have been utilized. The spectral data have been subjected to multivariate analysis to reveal major botanical origins and to correlate propolis composition to the altitude of its collection.

2. Materials and methods

2.1. Chemicals and samples

HPLC-grade methanol was obtained from Merck (Germany), and ultrapure water was obtained from a Milli-Q water system (Darmstadt, Germany). Dimethyl sulfoxide-d_6 was purchased from Sigma-Aldrich (St. Louis, MO, USA). This study is comprised of 59 propolis samples collected from February 2008 to October 2014, from 48 different hives located in Serbia, Bosnia and Herzegovina, and Bulgaria. The locations varied in elevation from 100 to 1000 m with temperate continental climate (Table 1). The buds of *Populus tremula*, *P. nigra*, and *P. x euramericana* were provided by the Institute of Lowland Forestry and Environment (Novi Sad, Serbia).

2.2. Preparation of extracts

Propolis samples (0.5 g) were cooled to -18°C, ground by mortar and pestle, and then extracted with 5 mL of methanol for 24 h in the dark. The samples were then cooled to -18°C for 1 h, and immediately filtered by a precooled funnel. The filtrates were then evaporated to dryness using a stream of nitrogen gas. The extracts were stored at -18°C until analysis. For the NMR measurements, 20 mg of the propolis extract was dissolved in 500 µL of dimethyl sulfoxide-d_6. Whole buds of *Populus* species (0.5 g) were extracted with 800 µL of dimethyl sulfoxide-d_6, using an ultrasonic bath for 5 min. The buds were then removed, and the extract was used for NMR measurements.

For the UV-Vis measurements, 3 µL of the solution obtained for NMR spectroscopy was diluted with 3 mL of methanol. The baseline for UV-Vis spectra, recorded from the solution, contained 3 µL of dimethyl sulfoxide-d_6 and 3 mL of methanol. The freeze-dried dimethyl sulfoxide-d_6 extracts were used for the FT-IR measurements.

2.3. General experimental procedures

NMR spectra were acquired on a Bruker Avance III 500 MHz instrument (Karlsruhe, Germany) with a 5 mm BBO probe, using standard pulse sequences. Dimethyl sulfoxide-d_6 was used as a solvent at a temperature of 289 K. The spectra were referenced to the residual solvent signal (δH 2.50, δC 39.51). Chemical shifts are given in δ (ppm), and coupling constants are reported in Hz. For the ^{1}H NMR spectra, 32k data points were collected, using a "zg30" pulse program with 128 scans, a spectral width of 8013 Hz, and a relaxation delay of 2 s. 2D *J*-resolved NMR spectra were acquired using 16 scans per 64 increments of F1 and 8k for F2.

IR spectra were recorded on a Thermo Scientific Nicolet 6700 FT-IR spectrometer, using the attenuated total reflectance (ATR) technique from the Smart accessory with diamond crystal (Smart Orbit, Thermo Scientific, Madison, WI, USA). Spectral data were collected in the mid-IR range (1800–600 cm^{-1}) with 64 scans and 2 cm^{-1} resolution. A background spectrum (32 scans) was recorded before every sample spectrum.

UV-Vis spectra were recorded using a GBC Cintra 40 UV/VIS spectrometer (Dandenong, Australia) in a range of 250 to 500 nm.

2.4. Data processing

1D and 2D NMR spectra were processed using TopSpin software version 3.2 (Bruker Biospin, Germany). The ^{1}H NMR spectra were manually phased and baseline corrected. The *J*-resolved spectra were tilted by 45º and symmetrized along F1. ^{1}H NMR spectra and 1D projections of 2D *J*-resolved spectra were binned using MestReNova software version 6.0.2 (Mestrelab Research, Santiago de Compostela, Spain). The spectra were reduced to integrated regions of equal width (0.04 ppm) corresponding to the region of δ 2.54–13.50, and exported to ASCII files.

IR spectra were baseline corrected and smoothed using OMNIC software (version 7.0, Thermo Scientific, USA), and exported to SPC files.

UV spectra were exported to DX files without processing.

Orthogonal partial least squares to latent structures (OPLS) and two-way orthogonal partial least squares (O2PLS) methods were performed with SIMCA software (version 14, Umetrics, Umeå, Sweden). Spectral data were normalized to total area, mean centered, and scaled to unit variance. In addition, the second derivative was applied for IR spectral data. For the ^{1}H NMR spectra and 1D projections of the 2D *J*-resolved spectra, the regions of δ 3.14 – 3.22 and δ 3.86 - 4.47 were excluded from the analysis because of the residual signal of methanol and water, respectively.

Spectral deconvolution was performed with OMNIC software version 7.0 (Thermo Scientific, USA). The whole spectral range (1800–600 cm^{-1}) was fitted using the Voigt function.

3. Results and discussion

3.1. Identification of the chemical compounds

For all the propolis samples, NMR, IR, and UV spectra were collected. Among the spectroscopic methods selected, 1D and 2D NMR techniques were the most powerful tool for elucidating the structure of propolis constituents. By visual inspection of ^{1}H NMR spectra, considerable differences have emerged between samples collected from different locations. The representative ^{1}H NMR, IR, and UV spectra of propolis originated from high (above 500 m) and low (below 400 m) in altitude are shown in Figure 1.

^{1}H NMR resonances were assigned to compounds by comparing the resonances with our in-house NMR spectroscopic database of phenolic compounds. Extensive analysis of 2D methods, including COSY, NOESY, TOCSY, HSQC, HMBC, and *J*-resolved (JRES) spectra allowed overlapping regions to be resolved in ^{1}H NMR spectra. The characteristic positions of 2D correlations were also compared with those from our database of pure compounds. ^{1}H NMR chemical shifts, multiplicity of the signals, and coupling constants were extracted from JRES spectra. NMR assignments were also confirmed by comparing the data with relevant information from the literature [31,32]. A total of 23 metabolites, including flavonoids, free phenolic acids, phenolic esters, and glycerides were identified, and the data are listed in Table 2.

Additionally, the main compounds in propolis samples were also detected by IR spectra. In order to distinguish between overlapping bands in the IR spectra of propolis and pure components, spectral deconvolution was applied. Characteristic bands were extracted from the IR spectra after deconvolution, and wavenumbers were then compared to those of pure compounds (see supplementary material). In this way, all characteristic bands present in the IR spectra of pure compounds were also found in the IR spectra of propolis samples (Table 3). Vibrational band assignments in the IR spectra were based on data from the literature [40-42]. The bands at 1760 to 1650 cm^{-1} were attributed to the stretching vibrations of the ester and flavonoid carbonyl groups, and those from 1650 to 1460 cm^{-1} were attributed to double bond and aromatic ring stretching vibrations. The numerous bands attributed to aromatic, C-H, and O-H in-plane deformation vibrations were found from 1460 to 1020 cm^{-1}. The strong bands at 1280 and 1160 cm^{-1} were attributed to C-O stretching vibrations of esters and phenols, respectively.

The UV spectra of propolis samples showed characteristic absorption bends, corresponding to superposition of UV spectra of the flavonoid constituents (mainly chrysin, galangin, pinocembrine, and pinobanksin 3-*O*-acetate), as well as phenolic glycerides and phenylpropanoid derivatives.

3.2. Changes of chemical composition of propolis in relation to the altitude of sample collection

To follow the variability in propolis sample composition in relation to the altitude of its collection, qualitative and quantitative measurements of all metabolites are needed. This approach is well-known in plant and human metabolomics studies, where ^{1}H NMR spectroscopy, in combination with multivariate analysis, is the method of choice. Despite having low sensitivity, NMR has an advantage over chromatographic methods, since the areas of ^{1}H NMR signals are proportional to the molar concentration of an analyte. Thus, the direct comparison of their concentrations is possible, instead of using calibration curves for each individual compound [43].

According to our NMR analysis, the chemical composition of propolis is rather complex, containing a variety of closely related structures with similar NMR features. Consequently, severe spectral overlaps appeared in ^{1}H NMR spectra, which led to difficulties in finding discriminating compounds after multivariate analysis. The spectral overlap could be overcome by applying 2D NMR methods, but most of them suffer from long acquisition times. Nevertheless, besides ^{1}H NMR, we also acquired 2D JRES NMR spectra of the propolis samples. For the purpose of multivariate analysis, the projections of the tilted and symmetrized JRES spectra were used (pJRES). The result of this procedure was that pJRES appeared like a homonuclear, broadband decoupled 1D spectrum. Unlike an ordinary 1D spectrum, each proton appeared as a single peak, regardless of the multiplicity of the original signal [44]. Moreover, the broad signals in ^{1}H NMR spectra arising from exchangeable protons were absent in pJRES, resulting in flat baselines. Such simplified and baseline flattened pJRES spectra were therefore more appropriate for further multivariate analysis (Figure 2).

Orthogonal partial least squares to latent structures (OPLS) analysis was applied to correlate the spectral data (*X* variables) with the altitude of propolis collection (*Y* variables). The use of an orthogonal model separates the systematic variation in *X* into two parts: one linearly related to *Y* and one orthogonal to *Y*, which facilitates model interpretation [45].

According to the score plots of ^{1}H NMR and pJRES models, propolis samples collected at lower altitudes were clearly separated from those from higher altitudes (Figure 3). The OPLS models were validated by a permutation test (n = 200), and by cross validation-analysis of variance (CV-ANOVA). The goodness of fit of the models was described by R^2 (i.e., the fraction of Y variables explained by the model after cross validation), while Q^2 gave their predictive ability (Table 4). The high R^2 and Q^2 values revealed that NMR spectral data were related to the altitude of propolis collection. The pJRES model recorded higher R^2 and Q^2 values than the corresponding values obtained from ^{1}H NMR, which confirms that pJRES modeling is superior when overcoming severe spectral overlap. According to CV-ANOVA, both NMR-based OPLS models were significant with $p < 0.05$. This is in accordance with the results of the permutation test, where the regressions of Q^2 lines intersected the vertical axis below zero, and all the Q^2 and R^2 values of permuted *Y* vectors were lower than original ones.

For the abovementioned reasons, pJRES was advantageous over ^{1}H NMR spectra; thus, the pJRES OPLS model was used to interpret the variables responsible for the differences in propolis samples collected at various altitudes. Model interpretation was based on VIP scores of the predictive components (VIPpred) [46]. Variables with VIPpred scores above 1 were considered to be important for separation. The highest VIPpred values were recorded for signals of chrysin, galangin, pinocembrine, pinobanksin 3-*O*-acetate, 1,3-di-*p*-coumaryl-2-acetyl-glycerol, 1,3-diferulyl-2-acetyl-glycerol, benzyl *p*-coumarate, and coniferyl benzoate. The S-line plot was used for enhanced visualization of predictive loading, which is presented in a form similar to the original spectra (Figure 3) [47]. According to the loading plot, the major compounds in propolis samples collected above 500 m were the phenolic glycerides, 1,3- di-*p*-coumaryl-2-acetyl-glycerol and 1,3- diferulyl-2-acetyl-glycerol, as well as phenylpropanoid derivatives, benzyl *p*-coumarate and coniferyl benzoate. The flavonoids, chrysin, galangin, pinocembrine, and pinobanksin 3-*O*-acetate, were dominant in propolis samples collected at low altitudes (below 400 m). In the samples collected at 400-500 m, variable amounts of flavonoids, phenylpropanoid derivatives, and phenolic glycerides were found.

OPLS models with high R^2 and Q^2 values have also been obtained with IR and UV spectral data (Table 4). Corresponding score plots confirmed the correlation of chemical composition of propolis to the altitude where it was collected. The S-line plots of IR- and UV-based OPLS models also revealed the signals of discriminating compounds (Figure 3), confirming the dominance of flavonoids in the propolis samples collected below 400 m, and phenolic glycerides and phenylpropanoid derivatives in the samples collected above 500 m.

The ^{1}H NMR, IR, and UV spectra of two propolis samples, collected at high and low altitudes, as well as the spectra of corresponding pure compounds are presented in the supplementary materials.

If one compares the spectral data of propolis samples obtained with various techniques, UV spectroscopy had limited ability for detailed structure elucidation, but was useful to detect changes on the level of compound classes (flavonoid, phenylpropanoid derivatives, and phenolic glycerides). Nevertheless, UV is cheap, fast, and easy-to-use, capable of differentiating between propolis with different chemical compositions. IR spectroscopy is also a rapid method, practically not needing any sample preparation if ATR is used for data acquisition. IR spectra were more sensitive to fine changes in chemical structure and possessed much more variables than in a UV spectrum of propolis, although the assignment of every band in IR spectra is impossible. However, this is not a limitation for using particular bands as good markers for the presence of characteristic compounds in propolis. NMR spectroscopy is the best choice for metabolite profiling, since the combination of various 2D techniques enabled structural elucidation of the main constituents in propolis extracts.

As stated in the introduction, several papers have dealt with various analytical techniques in combination with multivariate analysis to classify *Populus* type propolis according to its geographical origin. Composition of propolis samples can vary considerably, even if they are collected at relatively low distance from each other. Thus the knowledge about what geographical factor is decisive for propolis composition is desirable. Herein, we found that the critical geographical factor is the altitude of propolis collection. According to the correlation we found, it is possible to assume the chemical composition of *Populus* type propolis from the information about the altitude of its collection. This assumption can be easily verified by only running the UV spectrum of the propolis extract. For more detailed information on its chemical composition, IR or ^{1}H NMR spectroscopy is preferable. This could be of great importance for quality control in companies that produce propolis based preparations.

3.3. Determination of the botanical origin of propolis

Since significant differences were found in propolis composition between higher and lower altitudes, we aimed to correlate these differences with the botanical origin of propolis. We have collected and analyzed bud extracts of three of the most widespread *Populus* species growing in the vicinity of the propolis collection sites. Namely, *P. tremula* was the dominant *Populus* species at altitudes higher than 500 m, while *P. nigra* was found at altitudes less than 400 m. A hybrid species, *P. x euramericana,* was dominant in the plains (100 m), where it is widely cultivated. In order to establish the botanical origin of propolis, the spectral data of the samples were compared to those of *Populus* bud extracts. An O2PLS method was utilized to integrate two blocks of data. This method identifies joint variation between two datasets, and systematic variation which is unique to each dataset. For this purpose, ^{1}H NMR, IR, and UV data were used. JRES spectra of bud extracts were not recorded, because the amounts of samples were too low, and the acquisition would take too long. The *X* matrix consisted of the spectral data of propolis extracts, and the *Y* matrix included spectral data of bud extracts.

Using the ^{1}H NMR data, we obtained an O2PLS model with one predictive component, eight orthogonal in *X*, and seven orthogonal in *Y*. According to R^2X and R^2Y values, 42.3% of the variance in the ^{1}H NMR spectral data of the propolis extracts overlapped with 73.5% of the variance in the ^{1}H NMR spectral data of the bud extracts (Table 5). The O2PLS analysis of IR data gave a model with two predictive components, five orthogonal in *X*, and two orthogonal in *Y*. In this model, 60.6% of the variance in the propolis extracts spectral data overlapped with 83% of the variance in the IR spectral data of the bud extracts (Table 5). Similarly, a UV-based O2PLS model gave one predictive component, six orthogonal in *X*, and six orthogonal in *Y*, where 74.1% of the variance in the spectral data of the propolis extracts overlapped with 83.6% of the variance in the UV spectra of the bud extracts.

Models obtained with a high amount of joint information from the *X* and *Y* matrix indicated that the botanical origin of propolis collected at altitudes higher than 500 m was predominantly *P. tremula* buds, while *P. nigra* and *P. x euramericana* buds were the source of propolis collected at altitudes below 400 m.

The VIPpred scores greater than 1 in the O2PLS models served to identify the influential variables from joint variation. Thus, the variables assigned to the flavonoids, chrysin, galangin, pinocembrine, and pinobanksin 3-*O*-acetate, and the phenolic glycerides, 1,3- di-*p*-coumaryl-2-acetyl-glycerol and 1,3- diferulyl-2-acetyl-glycerol, were found to be important to identify the botanical origin. The abovementioned flavonoids could be regarded as markers for propolis originating from *P. nigra* and *P. x euramericana* buds, while the phenolic glycerides could be markers for propolis originating from *P. tremula* buds.

Spectral data of bud extracts contained more joint information than propolis extract data. According to VIP scores of the orthogonal components (VIPorth) in the O2PLS NMR model, most of the orthogonal variation in the propolis samples was due to wax residues. This is not surprising, since honeybees collect material from plants and mix it with wax in order to make propolis. Also, a small contribution of plants other than the studied *Populus* species for propolis production cannot be excluded. The typical ^{1}H NMR, IR, and UV spectra of high and low altitude propolis, together with corresponding buds of *Populus* species are shown in Figure 4.

To our knowledge, this is the first time that methods of multivariate data analysis and non-separation techniques have been used to correlate the chemical composition of propolis with the chemical composition of corresponding bud exudates, thus revealing botanical origins.

4. Conclusions

The utilization of various spectroscopic techniques, in combination with sophisticated multivariate analysis methods, was demonstrated to be a powerful tool to correlate propolis composition to altitude of collection and reveal its major botanical origin. OPLS methods were used to identify changes in the chemical composition of propolis, while O2PLS methods enabled the identification of the botanical origin of propolis.

Among the spectroscopic techniques used, UV has been shown to be a cheap, fast, and simple technique, capable of differentiating between propolis of different origins, but lacks the ability for detailed metabolite identification. IR spectroscopy was also a rapid and cost-effective method capable of identifying propolis origin, and offered more structural information on propolis composition than UV spectroscopy. The power of NMR spectroscopic methods in structure elucidation has been demonstrated, proving to be the best option if detailed information on propolis constituents is needed. The most suitable OPLS method for variable interpretation has been achieved using projections of the tilted and symmetrized 2D *J*-resolved NMR spectra, due to simplification of the spectral lines.

Eight compounds were identified as the most influential in the OPLS pJRES model: the phenolic glycerides, 1,3-di-*p*-coumaryl-2-acetyl-glycerol and 1,3-diferulyl-2-acetyl-glycerol; the phenylpropanoid derivatives, benzyl *p*-coumarate and coniferyl benzoate; and the flavonoids, chrysin, galangin, pinocembrine, and pinobanksin 3-*O*-acetate. According to OPLS and O2PLS, the major compounds in propolis samples collected above 500 m were phenolic glycerides, originating from *P. tremula* buds, while the flavonoids were predominant in propolis samples collected below 400 m, originating from *P. nigra* and *P. x euramericana* buds. The samples collected at 400-500 m were of mixed origin, with variable amounts of all detected metabolites.

Acknowledgments

This study was financially supported by the Serbian Ministry of Education and Science, Project No. 172053. The authors thank Dr. Veselin Maslak and Aleksandra Mitrović, Faculty of Chemistry at the University of Belgrade, for synthesis of coniferyl benzoate, and Jennifer Shing (Center for Drug Evaluation and Research, U.S. Food and Drug Administration) for manuscript editing.

References

1. M.L. Khalil, Biological activity of bee propolis in health and disease. Asian Pac. J. Cancer Prev. 7 (2006) 22–31.
2. M.P. Popova, V.S. Bankova, S. Bogdanov, I. Tsvetkova, C. Naydenski, G.L. Marcazzan, A.G. Sabatini, Chemical characteristics of poplar type propolis of different geographic origin. Apidologie. 38 (2007) 306–311.
3. L. Chunying, Z. Xiaoli, L. Yuanqian, S. Chengjun, J. Yan, W. Zhiyun, Determination of flavonoids in propolis-rich functional foods by reversed phase high performance liquid chromatography with diode array detection. Food Chem. 127 (2011) 314–320.
4. J. Bertrams, N. Kunz, M. Müller, D. Kammerer, F.C. Stintzing, Phenolic compounds as marker compounds for botanical origin determination of German propolis samples based on TLC and TLC-MS. J Appl. Bot. Food Qual. 86 (2013) 143–153.
5. V. Bankova, B. Trusheva, M. Popova, New developments in propolis chemical diversity studies (since 2000). In: Scientific Evidence of The Use of Propolis in Ethnomedicine, Orsolich, N. and I. Basic (Ed.). Transworld Research Network, Trivandrum, India. 2008, pp. 1–13.
6. M.A. Savka, L. Dailey, M. Popova, R. Mihaylova, B. Merritt, M. Masek, P. Le, S.R.M. Nor, M. Ahmad, A.O. Hudson, V. Bankova, Chemical Composition and Disruption of Quorum Sensing Signaling in Geographically Diverse United States Propolis, Evid-Based Compl. Alt. (2015), doi:10.1155/472593
7. S. Huang, C.P. Zhang, K. Wang, G.Q. Li, F.L. Hu, Recent Advances in the Chemical Composition of Propolis. Molecules 19 (2014) 19610–19632.
8. J.J. Veloz, N. Saavedra, A. Lillo, M. Alvear, L. Barrientos, L.A. Salazar, Antibiofilm activity of chilean propolis on Streptococcus mutans is influenced by the year of collection. Bio. Med. Research International (2015) 1–7.
9. K. Saleh, T. Zhang, J. Fearnley, D.G.A. Watson, Comparison of the Constituents of Propolis from Different Regions of the United Kingdom by Liquid Chromatography-High Resolution Mass Spectrometry using a Metabolomics Approach. Current Metabolomics. 3 (2015) 42–53.
10. M.B. Wilson, D. Brinkman, M. Spivak, G. Gardner, J.D. Cohen, Regional variation in composition and antimicrobial activity of US propolis against Paenibacillus larvae and Ascosphaera apis. J. Invertebr. Pathol. 124 (2015) 44–50.
11. T. Suleman, van S. Vuuren, M. Sandasi, A.M. Viljoen, Antimicrobial activity and chemometric modelling of South African propolis. J. Appl. Microbiol. 119 (2015) 981–990.
12. T. Zhang, R. Omar, W. Siheri, S. Al Mutairi, C. Clements, J. Fearnley, R.A. Edrada-Ebel, D. Watson, Chromatographic analysis with different detectors in the chemical characterisation and dereplication of African propolis. Talanta. 120 (2014) 181–190.

13. S.I. Falcao, N. Vale, P. Gomes, M.R.M. Domingues, C. Freire, S.M. Cardoso, M. Vilas-Boas, Phenolic Profiling of Portuguese Propolis by LC-MS Spectrometry: Uncommon Propolis Rich in Flavonoid Glycosides. Phytochem. Analysis. 24 (2013) 309–318.
14. C. Gardana, M. Scaglianti, P. Pietta, P. Simonetti, Analysis of the polyphenolic fraction of propolis from different sources by liquid chromatography-tandem mass spectrometry. J. Pharmaceut. Biomed. 45 (2007) 390–399.
15. S. Kumazawa, M. Yoneda, I. Shibata, J. Kanaeda, T. Hamasaka, T. Nakayama, Direct evidence for the plant origin of Brazilian propolis by the observation of honeybee behavior and phytochemical analysis. Chem. Pharm. Bull. 51 (2003) 740–742.
16. K. Midorikawa, A.H. Banskota, Y. Tezuka, T. Nagaoka, K. Matsushige, D. Message, A.A.G. Huertas, S. Kadota, Liquid chromatography-mass spectrometry analysis of propolis. Phytochemical Analysis. 12 (2001) 366–373.
17. M.K. Choudhari, S.A. Punekar, R.V. Ranade, K.M. Paknikar, Antimicrobial activity of stingless bee (Trigona sp.) propolis used in the folk medicine of Western Maharashtra. India. J. Ethnopharmacol. 141 (2012) 363–367.
18. H.I. Marquez, O. Cuesta-Rubio, F.M. Campo, P.A. Rosado, R.M.O. Porto, A.L. Piccinelli, L. Rastrelli, Studies on the Constituents of Yellow Cuban Propolis: GC-MS Determination of Triterpenoids and Flavonoids. J. Agr. Food Chem. 58 (2010) 4725–4730.
19. M.P. Popova, K. Graikou, I. Chinou, V.S. Bankova, GC-MS Profiling of Diterpene Compounds in Mediterranean Propolis from Greece. J. Agr. Food Chem. 58 (2010) 3167–3176.
20. F.M. Campo, O. Cuesta-Rubio, P.A. Rosado, R.M. De Oca Porto Marquez, I. Hernandez, A.L. Piccinelli, L. Rastrelli, GC-MS determination of isoflavonoids in seven red Cuban propolis samples. J. Agr. Food Chem. 56 (2008) 9927–9932.
21. M. Kartal, S. Kaya, S. Kurucu, GC-MS analysis of propolis samples from two different regions of Turkey. Z. Naturforsch C. 57 (2002) 905–909.
22. V. Bankova, A.S. Galabov, D. Antonova, N. Vilhelmova, B. Di Perri, Chemical composition of Propolis Extract ACF and activity against herpes simplex virus. Phytomedicine. 21 (2014) 1432–1438.
23. V.A. Isidorov, L. Szczepaniak, S. Bakier, Rapid GC/MS determination of botanical precursors of Eurasian propolis. Food Chem. 142 (2014) 101–106.
24. M. Popova, B. Trusheva, R. Khismatullin, N. Gavrilova, G. Legotkina, J. Lyapunov, V. Bankova, The triple botanical origin of Russian propolis from the Perm region, its phenolic content and antimicrobial activity. Nat. Prod. Commun. 8 (2013) 617–620.
25. H. Cheng, Z.H. Qin, X.F. Guo, X.S. Hu, J.H. Wu. Geographical origin identification of propolis using GC-MS and electronic nose combined with principal component analysis. Food Res. Int. 51 (2013) 813–822.
26. M. Popova, B. Trusheva, S. Cutajar, D. Antonova, D. Mifsud, C. Farrugia, V. Bankova, Identification of the plant origin of the botanical biomarkers of Mediterranean type propolis. Nat. Prod. Commun. 7 (2012) 569–570.
27. M. Maraschin, A. Somensi-Zeggio, S.K. Oliveira, S. Kuhnen, M.M. Tomazzoli, J.C. Raguzzoni, C.M. Zeri Ana, R. Carreira, S. Correia, C. Costa, M. Rocha, Metabolic Profiling and Classification of Propolis Samples from Southern Brazil: An NMR-Based Platform Coupled with Machine Learning. J. Nat. Prod. 79 (2016) 13–23.
28. D.G. Watson, E. Peyfoon, L. Zheng, D. Lu, V. Seidel, B. Johnston, J.A. Parkinson, J. Fearnley, Application of principal components analysis to ^{1}H-NMR data obtained from propolis samples of different geographical origin. Phytochem. Anal. 17 (2006) 323-331.
29. R.S.N. Paganotti, J.C. Rezende, P.J.S. Barbeira, Discrimination Between Producing Regions of Brazilian Propolis by UV-VIS Spectroscopy and Partial Least Squares Discriminant Analysis. Curr. Anal. Chem. 10 (2014) 537–544.

30. R. Cai, S. Wang, Y. Meng, Q. Meng, W. Zhao, Rapid quantification of flavonoids in propolis and previous study for classification of propolis from different origins by using near infrared spectroscopy. Anal. Methods-UK. 4 (2012) 2388–2395.
31. G. Papotti, D. Bertelli, M. Plessi, M.C. Rossi. Use of HR-NMR to classify propolis obtained using different harvesting methods. Int. J. Food Sci. Tech. 45 (2010) 1610–1618.
32. D. Bertelli, G. Papotti, L. Bortolotti, G.L. Marcazzan, M. Plessi, ¹H-NMR simultaneous identification of health-relevant compounds in propolis extracts. Phytochem. Anal. 23 (2012) 260–266.
33. O. Cuesta-Rubio, A.L. Piccinelli, M.C. Fernandez, I.M. Hernández, A. Rosado, L. Rastrelli, Chemical characterization of Cuban propolis by HPLC-PDA, HPLC-MS, and NMR: the brown, red, and yellow Cuban varieties of propolis. J. Agric. Food. Chem. 55 (2007) 7502-7509.
34. T. Chasset, T.T. Häbe, P. Ristivojević, G.E. Morlock, Profiling and classification of French propolis by combined multivariate data analysis of planar chromatograms and scanning direct analysis in real time mass spectra. J. Chromatogr. A. 2016 Sep 23;1465:197-204.
35. G.E. Morlock, P. Ristivojević, E.S. Chernetsova, Combined multivariate data analysis of high-performance thin-layer chromatography fingerprints and direct analysis in real time mass spectra for profiling of natural products like propolis; J. Chromatogr. A. 1328 (2014) 104–112.
36. D. Milojković Opsenica, P. Ristivojević, J. Trifković, I. Vovk, D. Lušić, Ž. Tešić, TLC Fingerprinting and Pattern Recognition Methods in the Assessment of Authenticity of Poplar-Type Propolis. J. Chromatogr. Sci. 54 (2016) 1077-1083.
37. P. Ristivojević, F.L. Andrić, J.Đ. Trifković, I. Vovk, L.Ž. Stanisavljević, Ž.L. Tešić, D. Milojković Opsenica, Pattern recognition methods and multivariate image analysis in HPTLC fingerprinting of propolis extracts; J. Chemom. 28 (2014) 301–310.
38. C. Sârbu, A.C. Moţ, Ecosystem discrimination and fingerprinting of Romanian propolis by hierarchical fuzzy clustering and image analysis of TLC patterns. Talanta. 85 (2011) 1112–1117.
39. I. Dimkić, P. Ristivojević, T. Janakiev, T. Berć, J. Trifković, D. Milojković-Opsenica, S. Stanković, Phenolic profiles and antimicrobial activity of various plant resins aspotential botanical sources of Serbian propolis. Ind. Crops Prod. 94 (2016) 856–871.
40. C.N.R. Rao, Chemical application of infrared spectroscopy. New York and London: Academic press, 1963. pp. 175–237.
41. R. Swisłocka, M. Kowczyk-Sadowy, M.W.L. Kalinowska, Spectroscopic (FT-IR, FT-Raman, 1H and 13C NMR) and theoretical studies of p-coumaric acid and alkali metal p-coumarates. Spectroscopy-US. 27 (2012) 35–48.
42. M. Heneczkowski, M. Kopacz, D. Nowak, A. Kuzniar, Infrared spectrum of some flavonoids. Acta Pol. Pharm. 58 (2001) 415–420.
43. H.K. Kim, Y.H. Choi, R. Verpoorte, NMR-based metabolomic analysis of plants. Nat. Protoc. 5 (2010) 536–549.
44. L. Christian, R.V. Mark, Two-dimensional J-resolved NMR Spectroscopy: Review of a Key Methodology in the Metabolomics Toolbox. Phytochem. Anal. 21 (2010) 22–32.
45. S. Wiklund, E. Johansson, L. Sjöström, E.J. Mellerowicz, U. Edlund, J.P. Shockcor, J. Gottfries, T. Moritz, J. Trygg, Visualization of GC/TOF-MS-Based Metabolomics Data for Identification of Biochemically Interesting Compounds Using OPLS Class Models. Anal. Chem. 80 (2008) 115–122.
46. B. Galindo-Prieto, L. Eriksson, J. Trygg, Variable influence on projection (VIP) for orthogonal projections to latent structures (OPLS). J. Chemometr. 28 (2014) 623–632.
47. L. Eriksson, T. Byrne, E. Johansson, J. Trygg, C. Wikström, Multi- and Megavariate Data Analysis Basic Principles and Applications. 3rd revised ed. Umetrics Academy, 2013. pp. 220–223

Figure captions

Fig. 1. Representative ^{1}H NMR, IR, and UV spectra of propolis originating from high (A) (above 500 m) and low (B) (below 400 m) altitudes

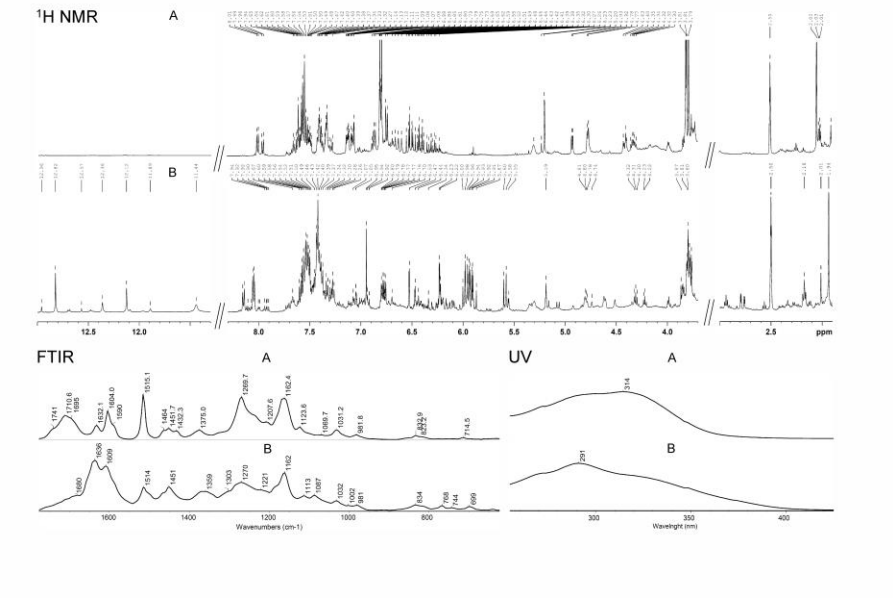

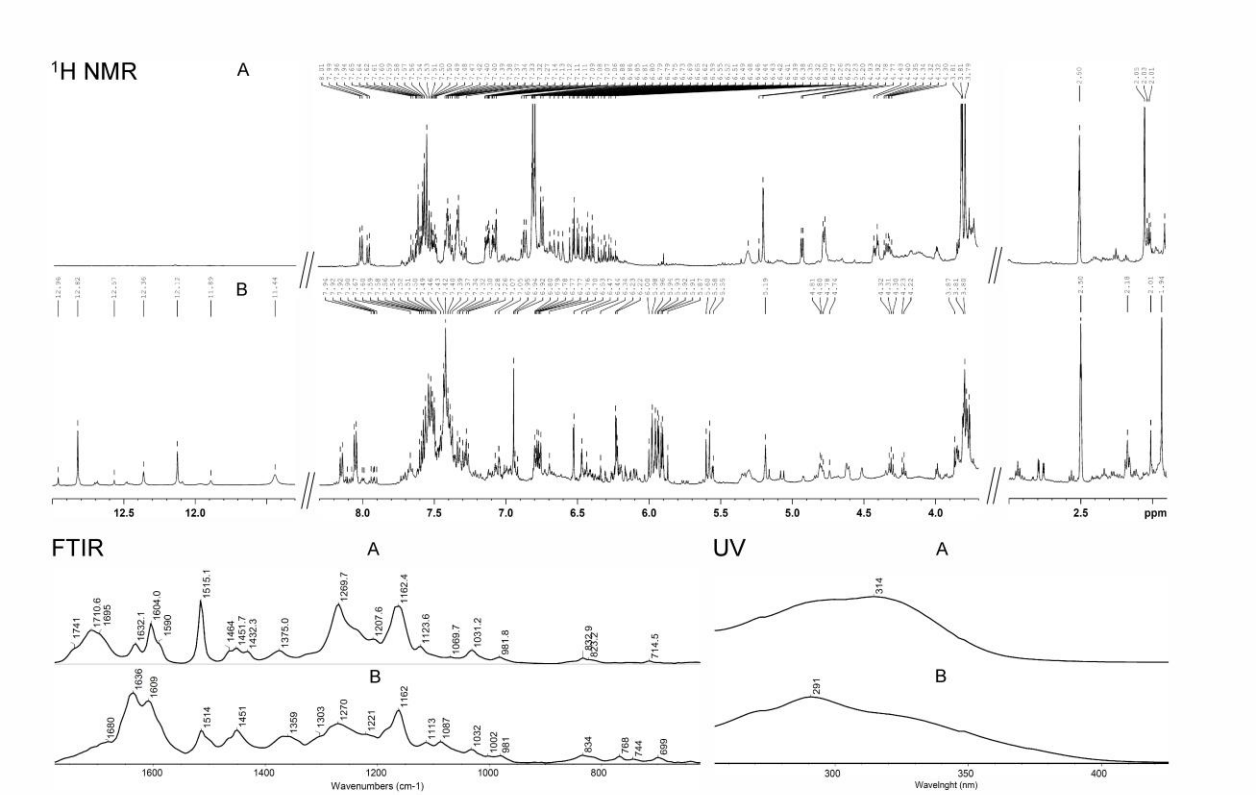
1H NMR
A
B
12.5
12.0
8.0
7.5
7.0
6.5
6.0
5.5
5.0
4.5
4.0
2.5
ppm
FTIR
A
1741
1710.6
1695
1632.1
1604.0
1590
1515.1
1464
1451.7
1432.3
1375.0
1269.7
1207.6
1162.4
1123.6
1069.7
1031.2
981.8
832.9
823.2
714.5
B
1680
1636
1609
1514
1451
1359
1303
1270
1221
1162
1113
1087
1032
1002
981
834
768
744
699
1600
1400
1200
1000
800
Wavenumbers (cm-1)
UV
A
314
B
291
300
350
400
Wavelnght (nm)

Fig. 2. The projection of the tilted and symmetrized 2D *J*-resolved spectrum (pJRES), and ^{1}H NMR spectrum of the propolis extract

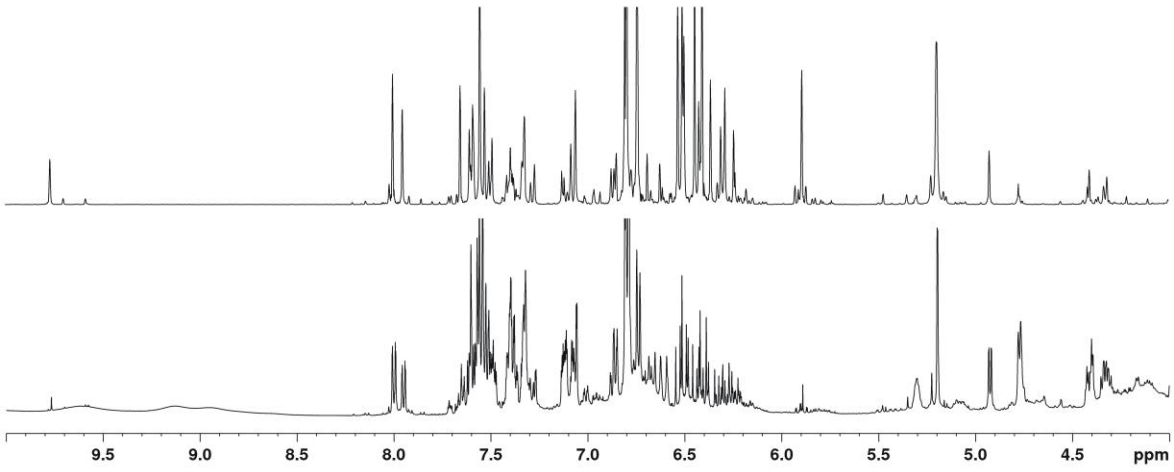

Fig. 3. Score plots and S-line plots of the ^{1}H NMR-, pJRES-, IR- and UV-based OPLS models considering propolis samples collected from various altitudes

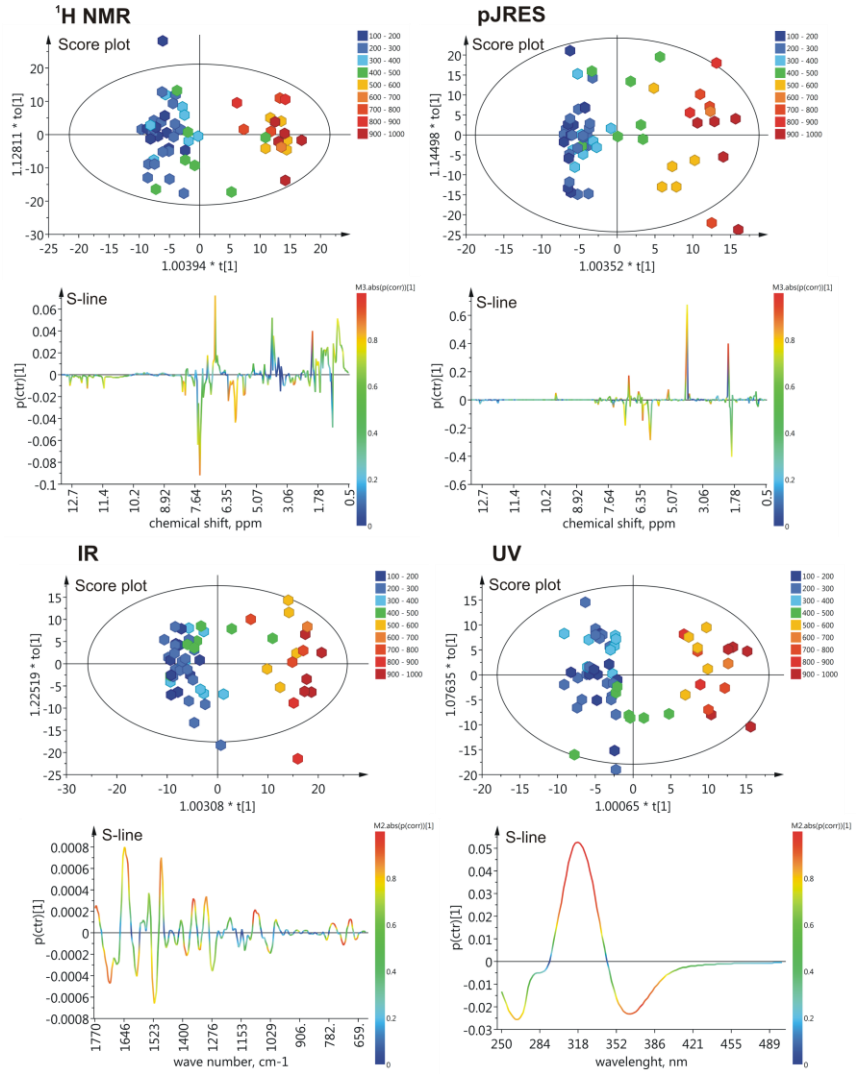

Fig. 4. Representative ^{1}H NMR, IR, and UV spectra of high (A) (above 500 m) and low altitude (B) (below 400 m) propolis, together with corresponding bud extract spectra of *Populus tremula* (PT) and *Populus x euramericana* (PE)

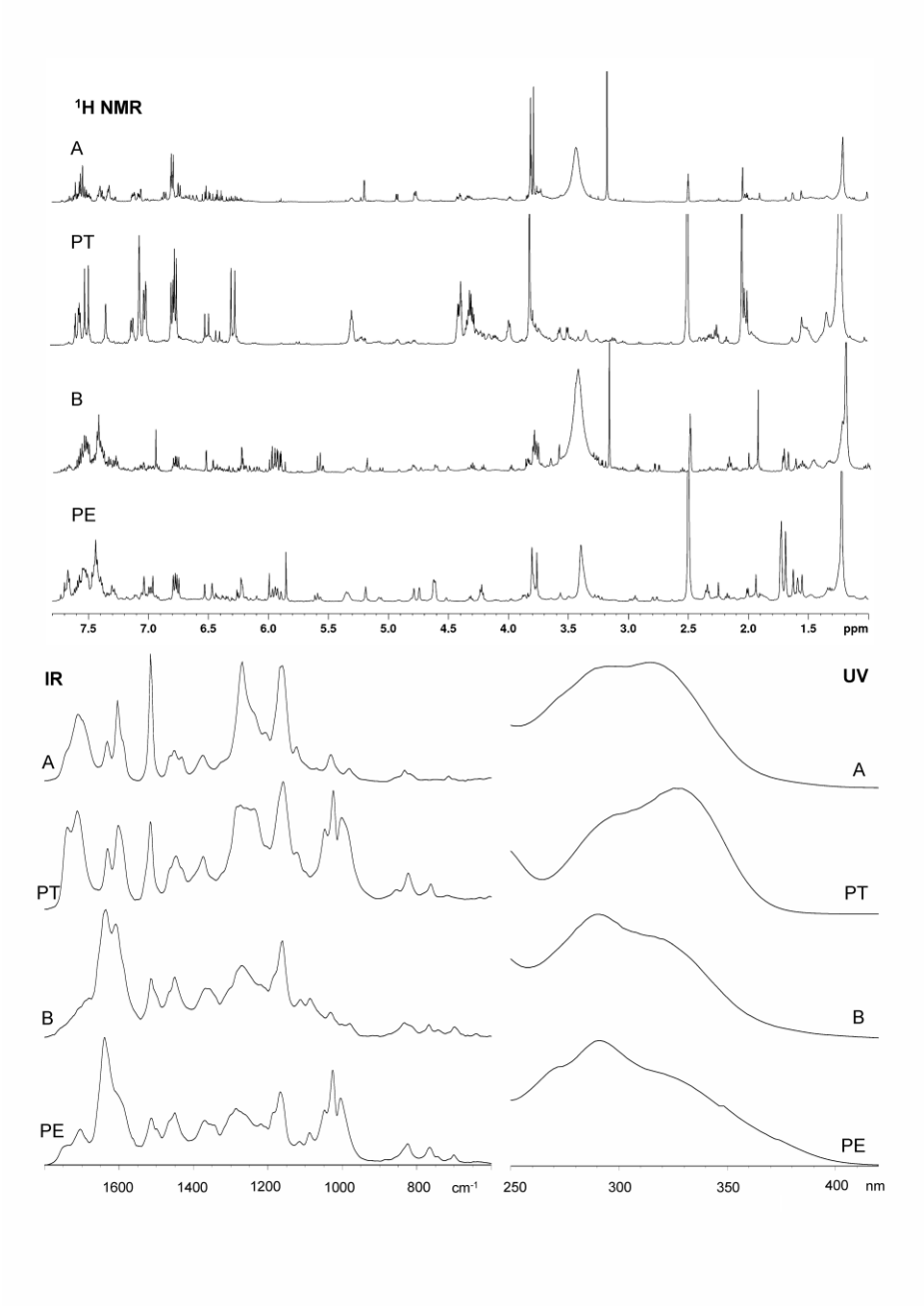

Table 1. Collection data of propolis samples

Number	Sampling time	Sampling locality	Altitude
1	Apr-13	Varvarin, Serbia	150
2	Apr-08	Irig, Serbia	200
3	Sep-08	Irig, Serbia	200
4	Jun-08	Kraljevo, Serbia	300
5	Feb-08	Rušanj I, Serbia	200
6	Feb-08	Rušanj II, Serbia	200
7	Aug-09	Rušanj I, Serbia	300
8	Aug-09	Rušanj II, Serbia	200
9	May-13	Rušanj I, Serbia	200
10	Nov-09	Kule, Ivanjica, Serbia	550
11	Mar-13	Kule, Ivanjica, Serbia	550
12	Aug-13	Kule, Ivanjica, Serbia	550
13	Apr-14	Kule, Ivanjica, Serbia	550
14	Aug-10	Veliki Šiljegovac, Kruševac, Serbia	200
15	Mar-13	Veliki Šiljegovac, Kruševac, Serbia	200
16	Sep-13	Veliki Šiljegovac, Kruševac, Serbia	200
17	Apr-13	Vukanja, Kruševac, Serbia	500
18	Dec-08	Kupinovo, Serbia	100
19	Apr-13	Čačak, Serbia	300
20	Jul-08	Knjaževac, Serbia	150
21	Jun-09	Zlatibor, Serbia	850
22	Jun-13	Deliblatska Peščara I, Serbia	200
23	Oct-13	Deliblatska peščara I, Serbia	200
24	May-14	Deliblatska Peščara II, Serbia	200
25	May-14	Deliblatska Peščara III, Serbia	200
26	May-14	Deliblatska Peščara IV, Serbia	200
27	Jul-13	Vranje, Serbia	300
28	Apr-13	Novi Sad, Serbia	150
29	Jun-13	Grevci, Kruševac, Serbia	300
30	Mar-13	Homolje, Serbia	700
31	Mar-13	Blagoevgrad, Bulgaria	300
32	Apr-13	Dobrinje, Petrovac na Mlavi, Serbia	300
33	Sep-13	Užice - Ribašina, Serbia	400
34	May-13	Kalna, Serbia	300
35	Mar-13	Stara Pazova - Belegiš, Serbia	200
36	Oct-13	Stara Pazova, Serbia	200
37	Oct-08	Sjetovac, Bosanski Brod, Bosnia and Herzegovina	150

38	Oct-13	Kovin, Serbia	100
39	Apr-14	Banatski Karlovac I, Serbia	150
40	Apr-14	Banatski Karlovac II, Serbia	150
41	Apr-14	Banatski Karlovac III, Serbia	200
42	Sep-13	Banja kod Aranđelovca, Serbia	250
43	Apr-14	Prijepolje, Serbia	400
44	Apr-14	Kamena Gora, Prijepolje, Serbia	900
45	Sep-14	Koševine, Prijepolje, Serbia	450
46	Sep-13	Prijepolje, Serbia	400
47	Apr-14	Divci, Prijepolje, Serbia	450
48	May-14	Bela Crkva, Serbia	200
49	Apr-14	Sopotnica, Prijepolje, Serbia	900
50	Apr-14	Međani, Prijepolje, Serbia	900
51	Apr-14	Miljevići I, Prijepolje, Serbia	700
52	Apr-14	Miljevići II, Prijepolje, Serbia	700
53	Sep-14	Babine, Prijepolje, Serbia	1000
54	Sep-14	Purića potok, Prijepolje, Serbia	400
55	Sep-14	Kosatica, Prijepolje, Serbia	800
56	Sep-14	Miloševo, Prijepolje, Serbia	600
57	Sep-14	Zalug, Prijepolje, Serbia	400
58	Sep-14	Zvijezda, Prijepolje, Serbia	900
59	Oct-14	Kikinda, Serbia	150

Table 2. NMR data of the metabolites identified in the propolis samples.

Identified compound	Chemical shifts (ppm)
Chrysin	δ 12.82 (s), δ 8.05 (m), δ 7.56 (m), δ 6.95 (s), 6.53 (d, *J* = 2.0Hz), δ 6.23 (d, *J* = 2.0Hz).
Galangin	δ 12.36 (s), δ 8.15 (m), δ 7.52 (m), 6.47 (d, *J* = 2.0 Hz), δ 6.22 (d, *J* = 2.0 Hz).
Pinobanksin	δ 11.89 (s), δ 7.52 (m), δ 7.41 (m), δ 5.90 (br s), 5.87 (br s), δ 5.17 (d, *J* = 11.3 Hz), δ 4.61 (d, *J* = 11.3 Hz).
Pinocembrin	δ 12.12 (s), δ 7.52 (m), δ 7.41 (m), 5.93 (d, *J* = 2.2 Hz), δ 5.91 (d, *J* = 2.2 Hz), δ 5.57 (dd, *J* = 12.3, 2.8 Hz), δ 3.23 (dd, *J* = 17.1, 12.7 Hz), δ 2.78 (dd, *J* = 17.1, 2.8 Hz).
Pinobanksin 3-O-acetate	δ 11.44 (s), δ 7.53 (m), δ 7.43 (m), δ 5.98 (d, *J* = 2.2 Hz), 5.95 (d, *J* = 2.2 Hz), δ 5.93 (d, *J* = 11.8 Hz), 5.59 (d, *J* = 11.8 Hz), δ 1.94 (s).
Pinobanksin 3-O-methyleter	δ 7.49 (m), δ 7.40 (m), δ 6.11 (d, *J* = 2.1 Hz), 5.95 (d, *J* = 2.1 Hz), δ 5.07 (d, *J* = 11.8Hz), 4.33 (d, *J* = 11.8Hz), δ 3.77 (s).
Kaempheride	δ 12.69 (s), δ 7.91 (d, *J* = 9.0 Hz), δ 6.93 (d, *J* = 9.0 Hz), 6.35 (d, *J* = 2.2 Hz), δ 6.09 (d, *J* = 2.2 Hz), δ 3.77 (s).
Apigenin	δ 12.96 (s), δ 7.93 (d, *J* = 9.1 Hz), δ 6.95 (d, *J* = 9.1 Hz), 6.76 (s), δ 6.48 (d, *J* = 2.0 Hz), δ 6.20 (d, *J* = 2.0 Hz).
Naringenin	δ 7.31 (AA'BB'), δ 6.79 (AA'BB'), δ 5.89 (S), δ 5.43 (dd, *J* = 12.6, 2.8 Hz), δ 3.26 (dd, *J* =

	17.1, 12.6 Hz), δ 2.68 (dd, *J* = 17.1, 2.8 Hz).
Caffeic acid	δ 7.42 (d, *J* = 16.0 Hz), δ 7.05 (d, *J* = 1.8 Hz), 6.98 (dd, *J* = 8.1, 1.8 Hz), δ 6.77 (d, *J* = 8.1 Hz), δ 6.18 (d, *J* = 16.0 Hz).
Benzyl caffeate	caffeate moiety: δ 7.52 (d, *J* = 15.9 Hz), δ 7.05 (d, *J* = 1.8 Hz), 7.00 (dd, *J* = 8.1, 1.8 Hz), δ 6.76 (d, *J* = 8.1 Hz), δ 6.32 (d, *J* = 15.9 Hz). benzyl moiety: 7.38 (m), 5.19 (s).
Caffeic acid phenethyl ester	caffeic acid moiety: δ 7.52 (d, *J* = 15.9 Hz), δ 7.04 (d, *J* = 1.8 Hz), 7.01 (dd, *J* = 8.1, 1.8 Hz), δ 6.79 (d, *J* = 8.1 Hz), δ 6.32 (d, *J* = 15.9 Hz). phenethyl moiety: δ 7.26 (m), δ 4.31 (t, *J* = 6.9 Hz), δ 2.94 (t, *J* = 6.9 Hz).
Cinnamyl caffeate	Caffeic moiety: δ 7.46 (d, *J* = 15.9 Hz), δ 7.05 (d, *J* = 1.8 Hz), 7.01 (dd, *J* = 8.1, 1.8 Hz), δ 6.76 (d, *J* = 8.1 Hz), δ 6.25 (d, *J* = 15.9 Hz). Cinnamyl moiety: δ 7.46 (m), δ 6.71 (dt, *J* = 16.0, 1.8 Hz), δ 6.42 (dt, *J* = 16.0, 6.2 Hz), δ 4.80 (dd, *J* = 6.2, 1.8 Hz).
p-Coumaric acid	δ 7.51 (d, *J* = 8.2 Hz), δ 7.49 (d, *J* = 16.0 Hz), 6.78 (d, *J* = 8.2 Hz), δ 6.29 (d, *J* = 16.0 Hz).
Ferulic acid	δ 7.49 (d, *J* = 16.0 Hz), δ 7.27 (d, *J* = 2.0 Hz), 7.08 (dd, *J* = 8.1, 2.0 Hz), δ 6.79 (d, *J* = 8.1 Hz), δ 6.36 (d, *J* = 16.0 Hz), 3.81 (s).
Benzoic acid	δ 7.49 (dd, *J* = 8.6, 1.2 Hz), δ 7.61 (tt, *J* = 7.5, 1.2 Hz), δ 7.95 (dd, *J* = 8.6, 7.5 Hz).
Conyferyl benzoate	benzoate moiety: δ 8.00 (dd, *J* = 8.6, 1.2 Hz), δ 7.65 (tt, *J* = 7.5, 1.2 Hz), δ 7.53 (dd, *J* = 8.6, 7.5 Hz). conyferyl moiety: δ 7.08 (d, *J* = 1.9 Hz), δ 6.87 (dd, *J* = 8.1, 1.9 Hz), δ 6.75 (d, *J* = 8.1 Hz), δ 6.67 (dt, *J* = 15.9, 1.8 Hz), δ 6.31 (dt, *J* = 15.9, 6.5 Hz), δ 4.93 (dd, *J* = 6.5, 1.8 Hz), 3.79 (s).
Conyferyl *p*-coumarate	*p*-coumarate moiety: δ 7.60 (d, *J* = 15.8 Hz), δ 7.55 (d, *J* = 8.2 Hz), 6.80 (d, *J* = 8.2 Hz), δ 6.53 (d, *J* = 15.8 Hz). conyferyl moiety: δ 7.05 (d, *J* = 1.9 Hz), δ 6.86 (dd, *J* = 8.1, 1.9 Hz), δ 6.74 (d, *J* = 8.1 Hz), δ 6.61 (dt, *J* = 15.9, 1.8 Hz), δ 6.24 (dt, *J* = 15.9, 6.5 Hz), δ 4.77 (dd, *J* = 6.5, 1.8 Hz), 3.79 (s).
Benzyl *p*- coumarate	*p*-coumarate moiety: δ 7.58 (d, *J* = 16.0 Hz), δ 7.53 (d, *J* = 8.2 Hz), 6.80 (d, *J* = 8.2 Hz), δ 6.49 (d, *J* = 16.0 Hz). benzyl moiety: δ 7.35-7.43 (m), δ 5.20 (AB).
Benzyl ferulate	ferulate moiety: δ 7.60 (d, *J* = 16.0 Hz), δ 7.32 (d, *J* = 2.0 Hz), 7.13 (dd, *J* = 8.1, 2.0 Hz), δ 6.80 (d, *J* = 8.1 Hz), δ 6.41 (d, *J* = 16.0 Hz), 3.81 (s). benzyl moiety: δ 7.35-7.43 (m), δ 5.23 (br s).
1,3-diferulyl-2-acetyl-glycerol	ferulyl moiety: δ 7.59 (d, *J* = 16.0 Hz), δ 7.32 (d, *J* = 2.0 Hz), 7.13 (dd, *J* = 8.1, 2.0 Hz), δ 6.80 (d, *J* = 8.1 Hz), δ 6.50 (d, *J* = 16.0 Hz), 3.81 (s). 2-acetyl-glycerol moiety: δ 5.30 (m), δ 4.42 (dd, *J* = 12.0, 3.8 Hz), 4.33 (dd, *J* = 12.0, 6.1 Hz), δ 2.05 (s).
1-*p*-coumaryl-2-acetyl-3-ferulyl-glycerol	*p*-coumaryl moiety: δ 7.59 (d, *J* = 16.0 Hz), δ 7.49 (d, *J* = 8.1 Hz), 6.79 (d, *J* = 8.1 Hz), δ 6.4 (d, *J* = 16.0 Hz). ferulyl moiety: δ 7.59 (d, *J* = 16.0 Hz), δ 7.32 (d, *J* = 2.0 Hz), 7.12 (dd, *J* = 8.1, 2.0 Hz), δ 6.79 (d, *J* = 8.1 Hz), δ 6.50 (d, *J* = 16.0 Hz), 3.81 (s). 2-acetyl-glicerol moiety: δ 5.30 (m), δ 4.41 (m), 4.33 (m), δ 2.05 (s).
1,3-di-*p*-coumaryl -2-acetyl-glycerol	*p*-coumaryl moiety: δ 7.59 (d, *J* = 16.0 Hz), δ 7.55 (d, *J* = 8.1 Hz), 6.79 (d, *J* = 8.1 Hz), δ 6.4 (d, *J* = 16.0 Hz). 2-acetyl-glycerol moiety: δ 5.30 (m), δ 4.41 (dd, *J* = 12.0, 3.8 Hz), 4.33 (dd, *J* = 12.0, 6.1 Hz), δ 2.05 (s).

Table 3. The wavenumbers (cm^{-1}) of bands extracted after deconvolution from the IR spectra of propolis originating from high (A) and low (B) altitude, and corresponding pure compounds

Propolis A	Propolis B	1,3-Diferulyl-2-acetyl-glycerol	1,3-di-*p*-Coumaryl-2-acetyl-glycerol	Coniferyl benzoate	Benzyl *p*-coumarate	Pinobanksin 3-O-acetate	Pinocembrin	Chrysin	Galangin
1739	1761	1745	1743			1745			
1715		1717		1716					
	1710					1706	1706		
1694		1692		1693	1688				
	1690					1684			
1677				1679	1672				
	1657							1648	1660
1655				1655					
	1637					1634	1643		1634
1632		1632	1632	1629	1635				
1604	1608	1604		1600	1600	1599		1606	1607
1589	1585	1592	1594	1584	1588		1589	1578	
1557	1556		1558		1555	1560		1554	1563
1515	1514	1514	1515	1515	1517	1519			1522
1497	1497	1490	1496	1503	1501	1493	1498	1502	1494
1465	1469		1460		1462	1466	1466		1473
1446	1447	1446	1450	1453	1443	1448	1448	1447	1452
1432			1429	1428					
	1419							1423	
	1412						1410		1411
1376	1376	1377	1378	1375	1376	1380	1375	1374	1375
	1356							1355	
1321		1327	1325		1326				
1311	1309				1311	1310	1318	1312	1315
	1300						1299		
1281	1283		1280		1282	1282			1286
	1277						1276	1275	
1270		1271		1270					
	1259					1257			1260
1237		1237		1239	1232				
1207	1203	1203		1208	1204	1207		1200	1197
	1161						1164	1168	1165
1158			1159	1158	1149				

1103		1107			1103				
	1115					1116	1122	1123	1125
1100	1103		1097	1099				1103	1095
	1081					1087	1088		
	1077							1077	
1070				1069					
	1034								1034
1031	1026	1024	1027	1028		1023	1025	1028	
995	999		995	996		997	994	998	
981	979	980			982			970	973
	914					908		909	
	878					882		874	881
817			821	826	823				
760	767		768		755	763	773		768
	756							755	
							722	724	
714			710	713					
698	699				697	698	702	696	701
	679							674	
	641						640	642	636

Table 4. Overview of OPLS models

Method	Component (predictive+orthogonal)	R^2	Q^2	p (CV-ANOVA)
^{1}H NMR	1+1	0.791	0.724	3.02×10^{-14}
pJRES	1+2	0.905	0.811	3.97×10^{-17}
IR	1+1	0.828	0.772	1.01×10^{-16}
UV	1+1	0.817	0.779	8.84×10^{-17}

Table 5. Overview of O2PLS models

Method	Component[1]	R^2X *p*redictive	R^2X orthogonal in X		R^2Y predictive	R^2Y orthogonal in Y	Q^2
^{1}H NMR	1+8+7	0.423	0.264		0.735	0.261	0.628
IR	2+5+2	0.606	0.344		0.830	0.140	0.551
UV	1+6+6	0.741	0.256		0.836	0.163	0.682

[1] predictive + orthogonal in X + orthogonal in Y